

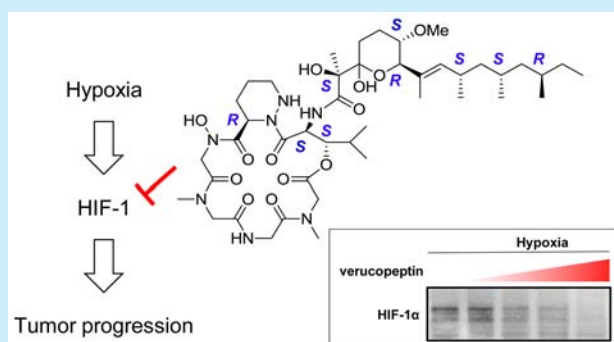
# Structure Elucidation of Verucepeptin, a HIF-1 Inhibitory Polyketide–Hexapeptide Hybrid Metabolite from an Actinomycete

Aya Yoshimura, Shinichi Nishimura, Saori Otsuka, Akira Hattori, and Hideaki Kakeya\*

Department of System Chemotherapy and Molecular Sciences, Division of Bioinformatics and Chemical Genomics, Graduate School of Pharmaceutical Sciences, Kyoto University, Sakyo-ku, Kyoto 606-8501, Japan

## Supporting Information

**ABSTRACT:** The transcriptional factor, hypoxia inducible factor-1 (HIF-1), is a promising target for cancer chemotherapy. From an actinomycete, verucepeptin (**1**) was identified as a HIF-1 signaling inhibitor. By a combination of chemical degradation and spectroscopic analyses, the absolute stereochemistry of metabolite **1** was determined to be 10R, 15S, 16S, 23S, 27S, 28R, 31S, 33S, 35R. Moreover, metabolite **1** was revealed to attenuate the HIF-1 $\alpha$  and mTORC1 pathway, indicating that verucepeptin (**1**) would be a potent lead compound for anticancer chemotherapy.



Adaptation to hypoxic environments is one of the characteristic features of tumor cells. HIF-1, a key transcription factor for tumor survival, regulates the expression of more than 800 genes, leading to diverse phenotypes for adaptation to and escape from the harsh environment, e.g., metabolic modulation, angiogenesis, invasion, and metastasis.<sup>1,2</sup> The activity of HIF-1, a heterodimer composed of HIF-1 $\alpha$  and HIF-1 $\beta$ , depends on HIF-1 $\alpha$  because this protein is degraded in an O<sub>2</sub>-dependent manner. Under normoxic conditions, two proline residues in HIF-1 $\alpha$  are hydroxylated by prolyl hydroxylase, which recruits von Hippel–Lindau tumor suppressor (pVHL) E3 ligase leading to degradation of HIF-1 $\alpha$  by the ubiquitin–proteasome pathway. Under hypoxic conditions, HIF-1 $\alpha$  is neither hydroxylated nor degraded, enabling the formation of the HIF-1 complex with HIF-1 $\beta$  in the nucleus. In contrast, transcription and translation of HIF-1 $\alpha$ , which is regulated by mammalian target of rapamycin complex 1 (mTORC1), is independent of the O<sub>2</sub> concentration.<sup>3</sup> It has been noted that tumor growth, vascularization, and metastasis correlate with the level of HIF-1 $\alpha$  both in animal models and in clinical studies.<sup>2</sup> Furthermore, dysfunction of proteins involved in the HIF-1 $\alpha$  degradation has been reported in some cancer cells.<sup>1</sup> For example, deficiency of pVHL was reported in renal carcinoma cells.<sup>4</sup> HIF-1 $\alpha$  is therefore one of the most promising targets for cancer chemotherapy.<sup>2,5</sup> However, there have been few reported compounds that show antitumor activity by selectively inhibiting HIF-1.<sup>6</sup>

To obtain novel HIF-1 modulators, we screened natural resources using a luciferase-reporter assay system<sup>7</sup> in which we could assess the effect of compounds on the transcriptional activity of HIF-1. We found that a culture broth of *Streptomyces* sp. KUSC\_A08 exhibited potent inhibitory activity in the reporter assay. Bioassay-guided fractionation of the culture

broth yielded verucepeptin (**1**) as an active constituent (Figure 1). Verucepeptin (**1**) was originally isolated as an antitumor compound from culture broth of the actinomycete *Actinomyces verrucosus*.<sup>8</sup> Metabolite **1** exhibited potent inhibitory activity in our reporter assay with an IC<sub>50</sub> value of 0.22

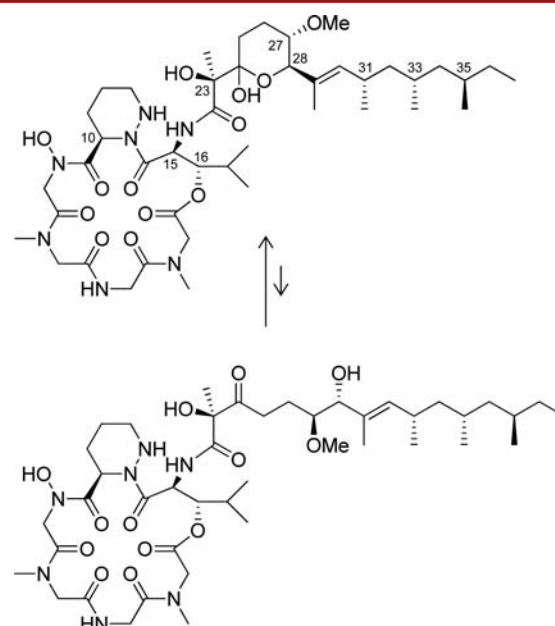


Figure 1. Chemical structure of verucepeptin (**1**).

Received: September 18, 2015

Published: October 20, 2015

$\mu\text{M}$ , whereas it showed cytotoxicity at concentrations above 1.1  $\mu\text{M}$  (Figure S1). Despite this potent biological activity, however, the absolute stereochemistry and its mode of action still required clarification.

Verucopeptin (1) is composed of a cyclic depsipeptide unit and a polyketide side chain.<sup>9</sup> The 19-membered cyclic depsipeptide consists of six amino acid residues, including one residue each of piperazic acid,  $\beta$ -hydroxy leucine, glycine, *N*-hydroxy glycine, and two *N*-methyl glycine residues. The absolute stereochemistry of the amino acids was determined by the Marfey's method.<sup>10</sup> Metabolite 1 was subjected to hydrogenolysis with  $\text{H}_2/\text{Pt}_2\text{O}$ , followed by acid hydrolysis and condensation with *L*- or *D*-FDAA. We compared the retention times of the FDAA derivatives with those of ornithine and synthesized  $\beta$ -hydroxy leucine diastereomers<sup>11</sup> on LCMS or HPLC, which revealed that piperazic acid and  $\beta$ -hydroxy leucine have the *D*- and *L*-*erythro* configurations, respectively (Figure S2). The amino acid configurations in the depsipeptide portion of verucopeptin (1) and its related metabolites seem to be conserved (Figure S3).

The side chain exhibits a dynamic equilibrium between a cyclic acetal form and a linear keto form (the ratio of keto and acetal form is 3:1 in  $\text{CDCl}_3$ ) (Figure 1).<sup>8</sup> We already reported the stereochemistry of the terminal portion of this polyketide chain; the 1,3,5-trimethylated system was determined to be 31*S*, 33*S*, 35*R* by degradation of the natural product, synthesis of the authentic compounds, and spectroscopic analysis.<sup>12</sup> To elucidate the stereochemistry of C23–C28, verucopeptin (1) was first reduced with  $\text{NaBH}_4$  to eliminate the natural equilibrium and yield two diastereomers. One diastereomer (2a) was purified by HPLC, and the resulting 1,2-diol function was protected with an isopropylidene group to obtain compound 3a (Figure 2a). In the NOESY spectrum of 3a, one of two methyl groups in isopropylidene, H24 and Me-38, showed a mutual correlation, indicating the *syn*-relationship of the diol (Figures 2b, S4a). The same approach was applied to the other diastereomer 2b, and the NOESY data obtained for 3b were consistent with the results obtained for compound 3a (Figure S4b). We next applied modified Mosher's analysis to determine the configurations of C-23 and C-28.<sup>13</sup> The *N*-hydroxyl group of the reduced product 2a was first protected, followed by reaction with (*S*/*R*)-MTPACl to yield bis(*R*/*S*)-MTPA derivatives 4a and 4b, respectively (Figure 2a). Analysis of the  $^1\text{H}$  NMR chemical shifts of 4a and 4b revealed the absolute stereochemistry of 24*S* and 28*R* (Figure 2c).<sup>14</sup> Taking these findings, the absolute stereochemistry of C23 and C28 was determined to be 23*S* and 28*R*, respectively.

The relative stereochemistry of C27 and C28 was deduced by the NMR data of verucopeptin (1) in the acetal form (Figure 3). In the ROESY spectrum, H28 showed correlations with H26a and H30, indicating that these hydrogen atoms are positioned on the same face. On the other hand, H27 showed ROESY correlations with H26a, H26b, and Me-40, indicating that these hydrogen atoms are located on the other face. This configuration was supported by the large coupling constant between H27 and H28 (9.8 Hz), which implied 27*S*\* and 28*R*\* stereochemistry. Since C-28 has an *R* stereochemistry, C-27 was deduced to be in an *S* configuration. Taken together, we unambiguously conclude that the absolute stereochemistry of verucopeptin (1) is 10*R*, 15*S*, 16*S*, 23*S*, 27*S*, 28*R*, 31*S*, 33*S*, 35*R* (Figure 1).

Verucopeptin (1) exhibited potent inhibitory activity in the HIF-1 reporter assay (Figure S1). Consistent with this result,

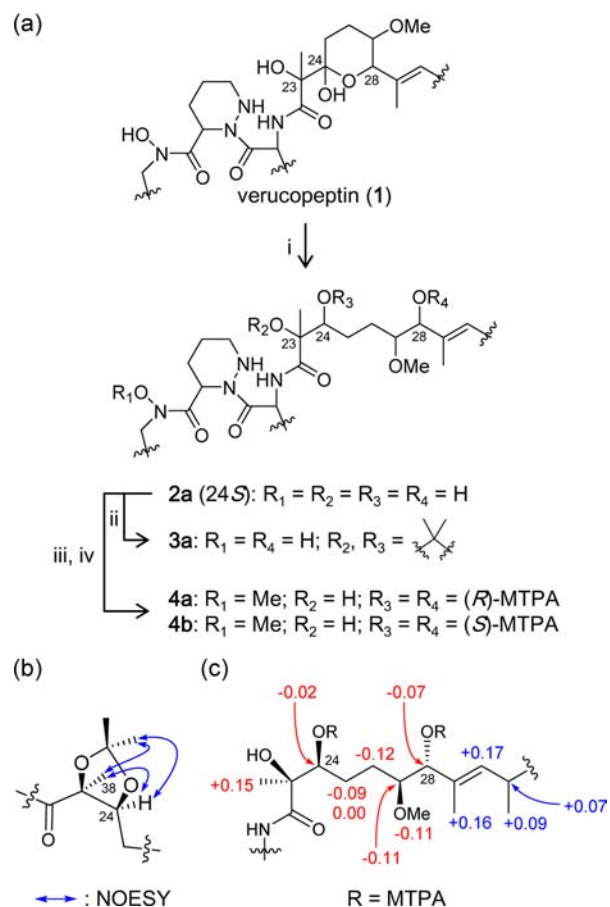


**Figure 2.** Determination of the absolute stereochemistry of C23 and C28 in verucopeptin (1). (a) Preparation of the isopropylidene derivative 3a and bis-MTPA derivatives 4a and 4b. (i)  $\text{NaBH}_4$ ,  $\text{MeOH}/\text{CH}_2\text{Cl}_2$ , rt, 0.5 h; (ii) 2,2-DMP, PPTS,  $\text{CH}_2\text{Cl}_2$ , rt, 1 h; (iii) MeI, TBAB,  $\text{K}_2\text{CO}_3$ ,  $\text{CH}_2\text{Cl}_2/\text{H}_2\text{O}$ , rt, 1 h; (iv) (*S*- or (*R*)-MTPACl, DMAP,  $\text{CH}_2\text{Cl}_2$ , rt, 1 h. Derivatives 2b and 3b are C24 epimers of 2a and 3a, respectively (see Supporting Information). (b) Selected NOESY correlations and relative structure of the 1,3-dioxolane structure in the isopropylidene derivative 3a. (c)  $\Delta\delta$  ( $\delta_{(S)\text{-MTPA}} - \delta_{(R)\text{-MTPA}}$ ) values for the MTPA derivatives 4a and 4b.  $\Delta\delta$  values are shown in ppm.

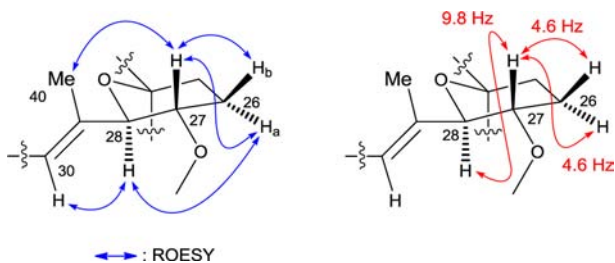


**Figure 3.** Determination of the relative stereochemistry of C27 in verucopeptin (1). ROESY correlations (left) and coupling constant values (right) in the tetrahydropyran ring are shown.

the endogenous mRNA levels of *glut1* and *bnip3*, HIF-1 target genes, was decreased by verucopeptin (1) in a concentration-dependent manner (Figures 4a, S6). Since there were no reports on the molecular mechanism underlying the antitumor activity of verucopeptin (1), we investigated the molecular mode of action. We first examined the mRNA and protein levels of HIF-1 $\alpha$ . When cells were treated with verucopeptin

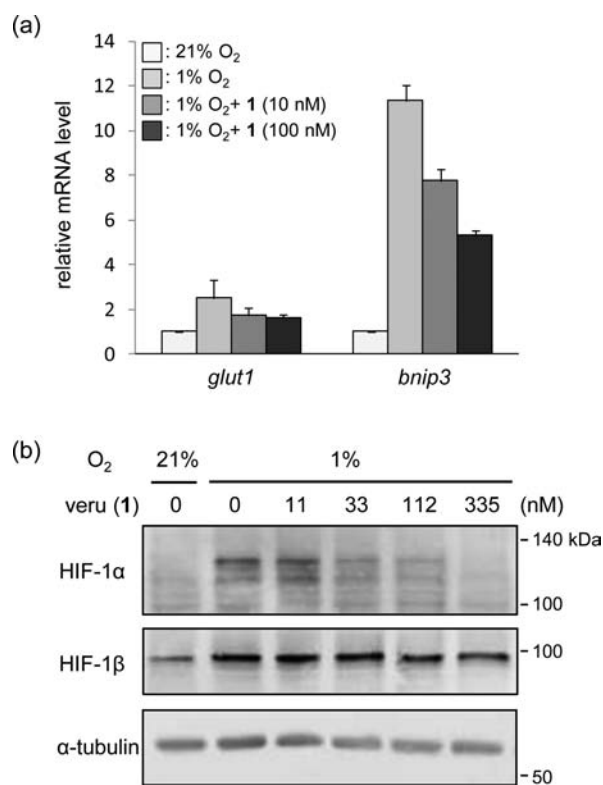


**Figure 4.** Effects of verucepeptin (**1**) on the transcriptional activity and protein level of HIF-1. (a) mRNA levels of *glut1* and *bnip3* in HT1080 cells were measured by qPCR ( $n = 4$ ). Cells were treated with verucepeptin (**1**) for 24 h in a hypoxic condition. (b) Effect of verucepeptin (veru; **1**) on the amount of HIF-1 $\alpha$  and HIF-1 $\beta$  proteins. HT1080 cells were treated with verucepeptin (**1**) for 24 h. Protein levels were detected by Western blot analysis.

(**1**), the mRNA level of HIF-1 $\alpha$  did not change (Figure S7); instead, the protein level of HIF-1 $\alpha$  decreased in a dose-dependent manner, whereas the protein level of HIF-1 $\beta$  was not affected (Figure 4b). These results implied that verucepeptin (**1**) might target stabilization or translation machineries of HIF-1 $\alpha$  protein.

HIF-1 $\alpha$  is a client protein of heat shock protein (HSP) 90; inhibition of HSP90 activity by 17-AAG, a well-known HSP90 inhibitor, moderately decreases the amount of HIF-1 $\alpha$ .<sup>15</sup> Notably, IC101, a microbial metabolite whose structure is related to verucepeptin (**1**), was reported to inhibit HSP90 functions at submicromolar concentrations.<sup>16</sup> To investigate whether verucepeptin (**1**) inhibits HSP90 in cells, we examined the amount of two client proteins, HIF-1 $\alpha$  and c-Raf. As expected, 17-AAG decreased the protein level of HIF-1 $\alpha$  and c-Raf (Figure S8). In contrast, the amount of c-Raf was not decreased in the presence of verucepeptin (**1**). These results indicated that HSP90 is not responsible for the effect of verucepeptin (**1**).

Translation of HIF-1 $\alpha$  has been reported to be regulated by the mTORC1 pathway through activation of p70S6K.<sup>3</sup> mTORC1 activates p70S6K by phosphorylation and p70S6K subsequently phosphorylates and activates S6 protein, a component of the ribosomal small subunit. To investigate the effect of verucepeptin (**1**) on the mTORC1 pathway, we detected the phosphorylation level of p70S6K and S6 proteins. We found that verucepeptin (**1**) attenuated the phosphorylation of S6 and S6K similar to the effect of rapamycin, an

mTORC1 inhibitor, suggesting that the mTORC1 pathway was blocked by verucepeptin (**1**) (Figure S9).

Rapamycin suppresses mTORC1 and HIF-1 $\alpha$  translation in some tumor cell lines.<sup>17</sup> Although the inhibitory activity of verucepeptin (**1**) against the mTORC1 pathway was less potent than that of rapamycin, we speculated that these two middle-sized molecules share target proteins. Rapamycin suppresses mTORC1 function by forming a ternary complex with FKBP12 and mTOR.<sup>18</sup> The binding site of rapamycin on FKBP12 is shared by another immunosuppressant FK506 and its substructure analog SLF. It was noted that SLF tightly bound to FKBP12,<sup>19</sup> but did not inhibit mTOR activity (Figure S10). As expected, the inhibition of phosphorylation of S6 protein by rapamycin was abolished by pretreating cells with an excess amount of SLF. However, the effect of verucepeptin (**1**) was not affected by SLF treatment (Figure S10). This result implied that the inhibition of p70S6K by verucepeptin (**1**) might not be mediated by FKBP12 or, at least, that verucepeptin (**1**) does not share the binding site on FKBP12 with rapamycin and SLF. Although we have not identified the cellular target(s) of verucepeptin (**1**), our data suggest that it targets mTORC1 itself, or the upstream components in the mTORC1 pathway (Figure S9). Alternatively, verucepeptin (**1**) might inhibit other pathways that indirectly suppress the mTORC1 pathway and HIF-1 $\alpha$  translation.

Verucepeptin (**1**) is a member of a family of 19-membered lipodepsipeptides (Figure S3).<sup>20</sup> This family of metabolites has been reported to exhibit unique biological activities. For example, azinothricin, A83586C, and kettapeptin show antibacterial activities against Gram-positive bacteria. Dentigerumycin, which is produced by *Pseudonocardia* sp. isolated from the cuticle of ants, strongly inhibits growth of parasitic fungus.<sup>21</sup> IC101 induces apoptosis by inhibiting HSP90 at submicromolar concentrations.<sup>16</sup> In our study, verucepeptin (**1**) was shown to inhibit the mTORC1 pathway, decrease the amount of HIF-1 $\alpha$  protein, and suppress the HIF-1 transcriptional activity. It was noted that the reduced derivative of verucepeptin (**2a**) showed significantly lower inhibition of HIF-1 transcriptional activity and cytotoxicity (Figure S1). The molecular basis underlying the diversity of these biological activities is of great interest.

In summary, we confirmed verucepeptin (**1**) as a new HIF-1 signaling inhibitor, determined its stereochemistry, and disclosed a unique mode of action. Chemical derivatization combined with a modified Mosher's method, advanced Marfey's method, and PGME method allowed us to deduce the absolute stereochemistry of verucepeptin (**1**). The stereochemistry of  $\beta$ -hydroxyleucine and piperazic acid was conserved among the congeners. Verucepeptin (**1**) decreased the expression of HIF-1 target genes and HIF-1 $\alpha$  protein levels, both of which correlated well with the inhibition of mTORC1 pathway components. These results indicated that verucepeptin (**1**), a new potent HIF-1 inhibitor, would be a promising lead compound for the development of novel antitumor drugs.

## ■ ASSOCIATED CONTENT

### Supporting Information

The Supporting Information is available free of charge on the ACS Publications website at DOI: 10.1021/acs.orglett.5b02718.

Experimental details, structure elucidation, and biological elucidation (PDF)

## AUTHOR INFORMATION

### Corresponding Author

\*E-mail: [sceigyo-hisyo@pharm.kyoto-u.ac.jp](mailto:sceigyo-hisyo@pharm.kyoto-u.ac.jp).

### Notes

The authors declare no competing financial interest.

## ACKNOWLEDGMENTS

We thank Dr. Hiroyuki Osada (RIKEN) for providing x5 HRE/HT1080 cells. This work was supported in part by research grants from the Project for Development of Innovative Research on Cancer Therapeutics (P-DIRECT) from the Japan Agency for Medical Research and Development (AMED), the Japan Society for the Promotion of Science (JSPS), the Ministry of Education, Culture, Sports, Science, and Technology of Japan (MEXT), and the Ministry of Health, Labour and Welfare of Japan (MHLW).

## REFERENCES

- (1) Semenza, G. L. *Annu. Rev. Pathol.: Mech. Dis.* **2014**, *9*, 47–71.
- (2) Semenza, G. L. *Trends Pharmacol. Sci.* **2012**, *33*, 207–214.
- (3) (a) Hudson, C. C.; Liu, M.; Chiang, G. G.; Otterness, M. D.; Loomis, C. D.; Kaper, F.; Giaccia, J. A.; Abraham, T. R. *Mol. Cell. Biol.* **2002**, *22*, 7004–7014. (b) Bian, C.-X.; Shi, Z.; Meng, Q.; Jiang, Y.; Liu, L.-Z.; Jiang, B.-H. *Biochem. Biophys. Res. Commun.* **2010**, *398*, 395–399.
- (4) Gunaratnam, L.; Morley, M.; Franovic, A.; de Paulsen, N.; Mekhail, K.; Parolin, A. E. D.; Nakamura, E.; Lorimer, A. J. I.; Lee, S. J. *Biol. Chem.* **2003**, *278*, 44966–44974.
- (5) Melillo, G. *Cancer Metastasis Rev.* **2007**, *26*, 341–352.
- (6) Keith, B.; Johnson, S. R.; Simon, C. M. *Nat. Rev. Cancer* **2011**, *12*, 9–22.
- (7) Yasuda, Y.; Arakawa, T.; Nawata, Y.; Shimada, S.; Oishi, S.; Fujii, N.; Nishimura, S.; Hattori, A.; Kakeya, H. *Bioorg. Med. Chem.* **2015**, *23*, 1776–1787.
- (8) (a) Nishiyama, Y.; Sugawara, K.; Tomita, K.; Yamamoto, H.; Kamei, H.; Oki, T. *J. Antibiot.* **1993**, *46*, 921–927. (b) Sugawara, K.; Toda, S.; Moriyama, T.; Konishi, M.; Oki, T. *J. Antibiot.* **1993**, *46*, 928–935.
- (9) Tsantrizos, Y. S.; Shen, J. H.; Trimble, L. A. *Tetrahedron Lett.* **1997**, *38*, 7033–7036.
- (10) (a) Fujii, K.; Ikai, Y.; Mayumi, T.; Oka, H.; Suzuki, M.; Harada, K. *Anal. Chem.* **1997**, *69*, 3346–3352. (b) Fujii, K.; Ikai, Y.; Oka, H.; Suzuki, M.; Harada, K. *Anal. Chem.* **1997**, *69*, 5146–5151. (c) Marfey, P. *Carlsberg Res. Commun.* **1984**, *49*, 591–596.
- (11) (a) MacMillan, B. J.; Molinski, F. T. *Org. Lett.* **2002**, *4*, 1883–1886. (b) MacMillan, B. J.; Ernst-Russell, A. M.; de Ropp, S. J.; Molinski, F. T. *J. Org. Chem.* **2002**, *67*, 8210–8215.
- (12) Yoshimura, A.; Kishimoto, S.; Nishimura, S.; Otsuka, S.; Sakai, Y.; Hattori, A.; Kakeya, H. *J. Org. Chem.* **2014**, *79*, 6858–6867.
- (13) Ohtani, I.; Kusumi, T.; Kashman, Y.; Kakisawa, H. *J. Am. Chem. Soc.* **1991**, *113*, 4092–4096.
- (14) We confirmed the 28R stereochemistry by another approach. Verucopeptin (**1**) was oxidatively cleaved by NaIO<sub>4</sub> and silica gel, yielding a lactone **S1**. The lactone **S1** was converted to a methyl ester **S2**, followed by the modified Mosher's analysis (Figure S5).
- (15) Dias, da R. S.; Friedlos, F.; Light, Y.; Springer, C.; Workman, P.; Marais, R. *Cancer Res.* **2005**, *65*, 10686–10691.
- (16) Fujiwara, H.; Yamakni, T.; Ueno, M.; Ishizuka, M.; Shinkawa, T.; Isobe, T.; Ohizumi, Y. *J. Pharmacol. Exp. Ther.* **2004**, *310*, 1288–1295.
- (17) Medici, D.; Olsen, R. B. *PLoS One* **2012**, *7*, e42913.
- (18) Fingar, C. D.; Blenis, J. *Oncogene* **2004**, *23*, 3151–3171.
- (19) Wu, X.; Wang, L.; Han, Y.; Regan, N.; Li, P.-K.; Villalona, A. M.; Hu, X.; Briesewitz, R.; Pei, D. *ACS Comb. Sci.* **2011**, *13*, 486–495.
- (20) (a) Maehr, H.; Liu, C.-M.; Palleroni, J. N.; Smallheer, J.; Todaro, L.; Williams, H. T.; Blount, F. J. *J. Antibiot.* **1986**, *39*, 17–25.
- (b) Smitka, A. T.; Deeter, B. J.; Hunt, H. A.; Mertz, P. F.; Ellis, M. R.; Boeck, D. L.; Yao, C. R. *J. Antibiot.* **1988**, *41*, 726–733. (c) Maskey, P. R.; Fotso, S.; Sevvana, M.; Usón, I.; Grünwollny, I.; Laatsch, H. *J. Antibiot.* **2006**, *59*, 309–314. (d) Ueno, M.; Amemiya, M.; Someno, T.; Masuda, T.; Iinuma, H.; Naganawa, H.; Hamada, M.; Ishizuka, M.; Takeuchi, T. *J. Antibiot.* **1993**, *46*, 1658–1665. (e) Hale, J. K.; Manaviyar, S.; George, J. *Chem. Commun.* **2010**, *46*, 4021–4042.
- (21) Oh, D.-C.; Poulsen, M.; Currie, R. C.; Clardy, J. *Nat. Chem. Biol.* **2009**, *5*, 391–393.